*energyequipsys/ Vol1/2013/*75-90

ENERGY EQUIPSYS

Energy Equipment and Systems

www.energyequipsys.com

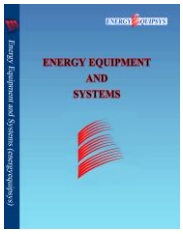

Study of the performance of a solar adsorption cooling system

Mahsa Sayfikar [a]
Ali Behbahani-nia [b*]

[a] M.Sc Student, Mechanical Engineering Department, K.N. Toosi University of Technology Tehran, Tehran, Iran

[b] Assistant Professor, Mechanical Engineering Department, K.N. Toosi University Of technology Tehran, Tehran, Iran

Article history:

Received 25 February 2013
Accepted 30 March 2013

ABSTRACT

This article presents a transient model of a solar adsorption cooling system. A computer program has been developed to simulate the operation of a two bed silica gel- water adsorption cooling system as well as flat plate collectors and the hot water storage tank. This program is then utilized to simulate the performance of a sample solar adsorption cooling system used for cooling a set of rooms that comprises an area of 52 m2 located in Ahwaz city in Iran. The system has been simulated with typical weather data of solar radiation and ambient temperatures of Ahwaz. The results include the temperature profiles of hot, cooling and chilled water in addition to Temperature profiles of adsorption/desorption beds, evaporator and condenser. Also the effects of the cycle time, switching time and hot water temperature on COP and refrigeration capacity are studied. Furthermore, the effects of solar collectors' surface area and the storage tank volume on total cost of the system are investigated in order to determine their optimum values able to maximize the overall thermo-economic performance of the system under analysis.

Keywords: Adsorption Cooling, Solar Energy, Solar Collectors.

1. Introduction

In recent years, considerable attention has been paid to adsorption refrigeration systems, which are regarded as environmentally friendly alternatives to conventional vapor compression refrigeration systems, since they can use refrigerants that do not contribute to ozone layer depletion and global warming. In addition, the adsorption systems have the benefits of simpler control, no vibration and lower operation costs, if compared with mechanical vapor compression systems. In comparison with the absorption systems, they do not need a solution pump or rectifier for the refrigerant, do not present corrosion problems due to the working pairs normally used, and are less sensitive to shocks and to the installation position [1]. Furthermore, refrigeration as a solar energy application is particularly attractive because of: 1) the non-dependence on conventional power and 2) the near coincidence of peak cooling loads with the solar energy availability.

Of course despite their many advantages, adsorption refrigeration systems present some drawbacks as well, such as low COP, low SCP, and high weight and high cost [1].

In the last three decades, extensive investigations on the performance of solar adsorption refrigeration/ heat pump systems have been conducted considering various adsorbent/ refrigerant pairs, such as activated carbon/ ammonia [2], zeolite/ water [3], activated carbon/ methanol [4] and silica gel/ water [5]. In general there are two types of solar adsorption cooling systems: 1) Integral systems in which the collector is used as the adsorber as well. And 2) Separated system in which the adsorber and collector are separated and a heat media is used to transfer heat from the collector to the adsorber.

The separated solar powered adsorption systems, can work more flexibly than the integral systems. The solar energy is unstable because of day–night alternation and cloud.

*Corresponding author:
Mechanical Engineering Department, K.N. Toosi University of Technology Tehran, Tehran, Iran
E-mail address: alibehbahaninia@kntu.ac.ir, (Ali Behbahaninia)

Therefore, an auxiliary heat source is necessary for a solar powered adsorption system to continuously yield cooling output. However, Most of the systems studied in the literature are integral systems, in which adsorption and cooling production can only be achieved during nights. Utilizing two bed adsorption chillers helps us overcome the intermittent character of solar adsorption refrigeration systems. In this context, silica gel-water was selected as the adsorbent–adsorbate pair. The potential for the two-bed silica gel-water adsorption chiller was evaluated by a number of researchers [6-8]. According to these studies, at a cooling temperature of 31°C and chilled water temperature of 14°C, a typical heating temperature is 85°C, while the lowest heat source temperature would be 70°C.

Since the adsorption/desorption processes in adsorbent beds are non-equilibrium. The adsorption/ desorption rate decreases with time, thus the energy input and output vary with time. On the other hand, solar energy is a typical variable heat source. The solar radiation condition is often affected greatly by season, weather and the time of day. Hence the fuel consumption in the auxiliary heater utilized in the solar system strongly fluctuates with time.

This paper presents the transient simulation of a solar two-bed silicagel-water continuous adsorption cooling system located in Ahwaz city in south west of Iran.(Fig.1) Also a parametric analysis is carried out to evaluate some optimal operating values of the system including hot water inlet temperature, cycle time, switching time, solar collector area and storage tank volume. Furthermore an economic analysis using Life cycle cost (LCC) method is performed in order to find the optimum values of collector area and storage tank volume.

2. Mathematical Model

2.1. Adsorption Chiller

Because the working principle of two bed adsorption chillers is elsewhere available in the literature [7,9] it will not be discussed here. A lumped parameter model is used in this study. The physical design parameters of the evaporator, condenser and adsorber/desorber heat exchangers are extracted from [6], which is a two-bed silicagel-water adsorption cooling system. All the parameters used in the chiller mathematical model are listed in Table 1. The main assumptions are taken as follows:

- The temperature and pressure are uniform throughout each adsorber.
- The system is well insulated thus has no heat losses to the environment.[6,7]
- The heat conduction of the shell connecting the adsorber to the condenser or the evaporator is neglected.
- The pressure difference between the adsorber and the condenser or the evaporator is neglected.

2.2. Adsorption Isotherm

The equilibrium uptake of silicagel- water pair is estimated using the equation developed by Boelman[10].

$$x^* = 0.346\left(\frac{P_s(T_w)}{P_s(T_s)}\right)^{1/1.6} \quad (1)$$

where $P_s(T_w)$ and $P_s(T_s)$ are respectively the corresponding saturated vapor pressures of the refrigerant at temperatures T_w (water vapor) and T_s(adsorbent). P_s for water vapor is estimated using the following equation:[6]

$$\begin{aligned} P_s = {} & 0.0000888(T-273.15)^3 \\ & -0.0013802(T-273.15)^2 \\ & +0.0857427(T-273.15) \\ & +0.4709375 \end{aligned} \quad (2)$$

2.2. Adsorption Kinetics

In the current chiller model the rate of adsorption or desorption is governed by the LDF equation [9] (Eq. (3)). The coefficients of LDF equation for silicagel-water are determined by Chihara and Suzuki [11] and are given in Table 1.

Table 1 parameters used in simulation of adsorption chiller.

Parameter	value
m_a	50 kg
ΔH_{ads}	2800kJ/kg
L	2500 kJ/kg
M_c	15.2kg
M_e	65.1kg
c_{cu}	0.386kJ/kgK
c_{pwv}	1.85kJ/kgK
c_{al}	0.905kJ/kgK
c_a	0.924kJ/kgK
c_{pw}	4.18kJ/kgK
M_{w0}	10kg
UA_e	3420W/K
UA_c	6090W/K
$UA_{heating}$	3570W/K
$UA_{cooling}$	3290W/K
m_{ad}	32.7kg
$\dot{m}_{hw}$	0.78kg/s
$\dot{m}_{cw}$	1.2kg/s
$\dot{m}_{chw}$	1kg/s
T_{chin}	15°C
T_{cin}	32.3°C
T_{hin}	85°C
D_{s0}	2.54E-4 m^2/s
R_p	1.7E-4 m
E_a	4.2E4 J/mol
F_0	15

$$\frac{\partial x}{\partial t} = k_s a_v (x^* - x) \quad (3)$$

$$k_s a_v = F_0 \frac{D_s}{R_p^2}, D_s = D_{s0} e^{-E_a/RT} \quad (4)$$

2.3. Energy Balance Equations

According to [7] in this study we assume that the relation $h_{ads}(T,P) = h_g(T,P) - \Delta H_{ads}$ holds at all times.

2.4. Energy Balance Equation for the Adsorption Beds:

Using the lumped approach, the energy balance equation for each bed is given by:

$$(m_{Hex}c_{al} + m_a c_a)\frac{dT}{dt} + m_a x c_{pw}\frac{dT}{dt} = \delta m_a \Delta H_{ads}\frac{dx}{dt} + \delta(1-\phi)m_a c_{pwv}\frac{dx}{dt}(T_e - T) + \dot{m}_w c_{pw}(T_{j,in} - T_{j,out}) \quad (5)$$

where the flag δ=0 during switching and δ=1 during adsorption/desorption cycle operation and j defines the cooling/heating source. Also depending on whether the bed adsorbs or desorbs the refrigerant, Φ would either be 0 or 1.

The outlet temperature of the heating water is modeled by the log mean temperature difference method and is given by:

$$\frac{T_{j,out} - T}{T_{j,in} - T} = \exp\left(-\frac{UA}{\dot{m}_w c_{pw}}\right) \quad (6)$$

2.5. Condenser Energy Balance

The condenser is a water cooled heat exchanger which liquefies the vapor refrigerant flowing from the desorbed during desorption, delivering the condensed liquid to the evaporator via a U tube. The energy balance equation for the condenser can be written as:

$$M_c c_{cu}\frac{dT_c}{dt} = m_a c_{pwv}\frac{dx_{des}}{dt}(T_c - T) - m_a \frac{dx_{des}}{dt}L + \dot{m}_{cw}c_{pw}(T_{cin} - T_{ccout}) \quad (7)$$

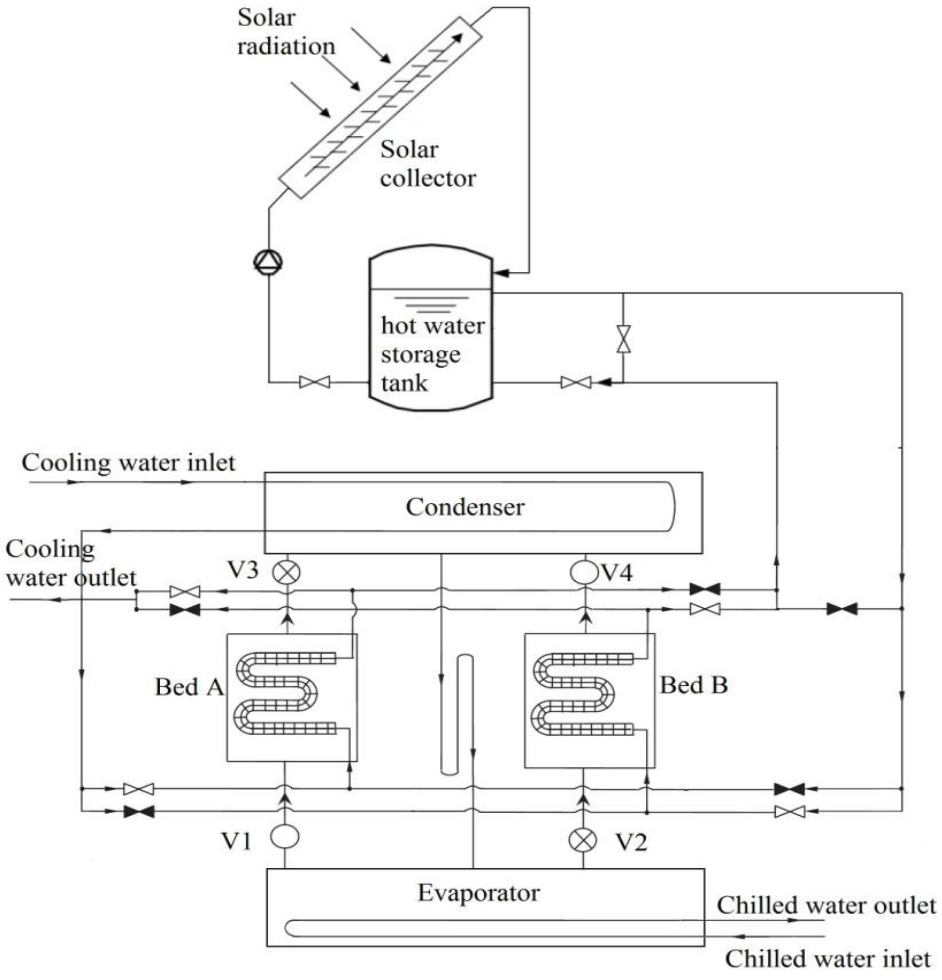

Fig.1. System layout.

2.6. Evaporator Energy Balance

The overall energy balance of the evaporator can be expressed as:

$$\begin{aligned}&(M_e c_{cu} + M_w(t) c_{pw}) \frac{dT_e}{dt} \\ &= -m_a \frac{dx_{ads}}{dt} L - m_a \frac{dx_{des}}{dt} c_{pw} \\ &\quad (T_c - T_e) + \dot{m}_{chw} c_{pw} (T_{chin} - T_{chout})\end{aligned} \quad (8)$$

where $M_w(t)$ is the amount of liquid water inside the evaporator at time t and is expressed by Eq.(9) :

$$M_w(t) = M_{w0} - m_a x_{ads} - m_a dx_{des} \quad (9)$$

The refrigeration capacity of this system is defined as:

$$\dot{Q}_e = \frac{\int_0^{\tau_{cycle}} \dot{m}_{chw} c_{pw} (T_{chin} - T_{chout}) dt}{t_{cycle}} \quad (10)$$

And the heating power required is:

$$\dot{Q}_h = \frac{\int_0^{\tau_{cycle}} \dot{m}_{hw} c_{pw} (T_{hin} - T_{hout}) dt}{t_{cycle}} \quad (11)$$

Hence COP can be expressed as:

$$COP = \frac{\dot{Q}_e}{\dot{Q}_h} \quad (12)$$

3. Solar Thermal System

The solar thermal system model includes a flat plate collector, a stratified storage tank and a back-up heater.

3.1. Solar Collectors

The solar collector is simulated using Eq.(13):

$$\begin{aligned}&\dot{m}_{sc} c_{pw} (T_{out,sc} - T_{in,sc}) = \\ &\qquad F_R(\tau\alpha) I_T A_c - F_R U_L A_c (T_{fi} - T_0)\end{aligned} \quad (13)$$

The available solar radiation data, which has been measured by Iran's meteorological organization, are the daily global solar radiations on a horizontal surface, daily sky clearness indexes and daily temperatures. It is necessary to have the instantaneous direct solar radiation that is received by the collector. The daily diffuse solar fraction is a function of sky clearness index (K_T) and is defined by Eq. (14): [12].

$$\frac{H_d}{H} = \begin{cases} 0.99 & for\ K_T \le 0.17 \\ 1.188 - 2.272K_T + 9.73K_T^2 & \\ -21.865K_T^3 + 14.648K_T^4 & for\ 0.17 \le K_T \le 0.75 \\ -0.54K_T + 0.632 & for\ 0.75 \le K_T \le 0.8 \\ 0.2 & for\ K_T > 0.8 \end{cases} \quad (14)$$

The instantaneous incident solar radiation on a tilted surface is the sum of a set of radiation streams including beam radiation, diffuse radiation and radiation reflected from other surfaces and is written as:

$$I_T = R_b I_b + I_d \left(\frac{1 - cos\beta}{2}\right) + I\rho_s \left(\frac{1 - cos\beta}{2}\right) \quad (15)$$

where the horizontal instantaneous global and diffuse radiations are obtained from the daily values by the following equations:

$$I = r_t \times H \quad (16)$$

$$r_t = \frac{\pi}{24}(a + b\cos\omega) \times \frac{\cos\omega - \cos\omega_s}{\sin\omega_s - \pi\frac{\omega_s}{180}\cos\omega_s} \quad (17)$$

$$\begin{aligned} a &= 0.409 + 0.5016\sin(\omega_s - 60) \\ b &= 0.6609 - 0.4767\sin(\omega_s - 60) \end{aligned} \quad (18)$$

$$I_d = r_d \times H_d \quad (19)$$

$$r_d = \frac{\pi}{24} \times \frac{\cos\omega - \cos\omega_s}{\sin\omega_s - \pi\frac{\omega_s}{180}\cos\omega_s} \quad (20)$$

$$I_b = I - I_d \quad (21)$$

and

$$R_b = \frac{\cos(\theta)}{\cos(\theta_z)} \quad (22)$$

$$\begin{aligned}\cos\theta &= \sin\delta\ sin\lambda\ cos\beta - \sin\delta\ cos\lambda\ sin\beta + \\ &\quad + \cos\delta\ cos\lambda\ cos\beta\ cos\omega \\ &\quad + \cos\delta\ sin\lambda\ sin\beta\ cos\omega\end{aligned} \quad (23)$$

$$\cos\theta_z = \cos\delta\cos\lambda\cos\omega + \sin\lambda\sin\delta \quad (24)$$

ρ_s is assumed to be 0.15 according to [12].

3.2. Storage Tank

The storage tank has 3 temperature nodes to simulate stratification. The collector injects heat into the storage tank, if the collector temperature is above the lowest storage tank temperature. The return to the collector is always taken from the bottom of the tank; the load supply is taken from the top of the tank. The collector outlet and the load return are put into the storage tank at the corresponding stratification temperature level. The energy balance on node i can be expressed as:

$$\begin{aligned}M_i c_{pw} \frac{dT_i}{dt} &= F_i^c \dot{m}_{co} c_{pw} (T_{co} - T_i) + \\ &\quad F_i^l \dot{m}_{lr} c_{pw} (T_{lr} - T_i) + UA_i (T_0 - T_i) + \\ &\quad \begin{cases} \dot{m}_{m,i} c_{pw} (T_{i-1} - T_i) if\ \dot{m}_{m,i} > 0 \\ \dot{m}_{m,i+1} c_{pw} (T_i - T_{i+1}) if\ \dot{m}_{m,i+1} < 0 \end{cases}\end{aligned} \quad (25)$$

where F_i^c, F_i^l and $\dot{m}_{m,i}$ are defined as:

$$F_i^c = \begin{cases} 1 \;\; if\; i = 1 \; and \; T_{co} > T_i \\ 1 \; if \; T_{i-1} \geq T_{co} > T_i \\ 0 \; if \; i = 0 \; or \; if \; i = 4 \\ 0 \qquad otherwise \end{cases} \tag{26}$$

$$F_i^l = \begin{cases} 1 \;\; if \; i = 3 \; and \; T_{lr} < T_N \\ 1 \qquad if \; T_{i-1} \geq T_{lr} > T_i \\ 0 \; if \; i = 0 \; or \; i = 4 \\ 0 \qquad otherwise \end{cases} \tag{27}$$

$$\dot{m}_{m,i} = \dot{m}_{co} \sum_{j=1}^{i-1} F_j^c - \dot{m}_{lr} \sum_{j=i+1}^{3} F_j^l \tag{28}$$

3.3. Auxiliary Heater

An auxiliary heater at the exit of the storage tank boosts the temperature of the hot water from the storage tank temperature to the reference temperature when the storage tank temperature drops below the allowable reference temperature.
The energy delivered to the water stream by the auxiliary heater is calculated using Eq.(29):

$$Q_{aux} = \dot{m}_{lr} . c_{pw} . \left(T_{auxh,out} - T_{auxh,in} \right) \tag{29}$$

In which $T_{auxh,out}$ is assumed to be 85°C.

3.4. Economic Analysis

In this study life cycle analysis (LCC) method is employed for economic analysis of the system. Investment costs of the solar cooling system include the price of solar collectors, storage tank, pumps, fans, ducts, pipes and adsorption chiller and are calculated using Eq.(30):

$$C_S = C_A A_c + C_E \tag{30}$$

where C_S is the total cost of installed solar energy equipment, C_A is the total area-dependent cost and C_E is the total cost of other equipment including adsorption chiller. C_A is calculated using:[13]

$$C_A = 121 + 1.107v \tag{31}$$

Since the objective of this analysis is to determine the optimal values of collector area and storage tank volume and these parameters have no effect on price of the chiller, the investment cost of adsorption chiller will not be included in calculations. Operational cost of solar adsorption (C_{NG}) system is simply calculated by multiplying the natural gas consumption with the unit price of the natural gas. Thus total LCC of the solar system can be calculated as follows:

$$LCC = C_A + \sum_{i=1}^{N} PW_i (C_{NG}) \tag{32}$$

where N is the lifetime of the solar-thermal cooling system in years. The time horizon and the discount rate were set to 20 years and 14% respectively and the unit cost of natural gas (c_{NG}) was assumed equal to 0.4959 $/m3.[13]

4. Simulation and Optimization Procedure

The energy balance equations of the major components such as adsorber/desorber beds, condenser and evaporator are solved by an iterative scheme, employing the Runge-Kutta method of order 3.A computer program written in MATLAB and based on this scheme has been developed in order to simulate the behavior of the adsorption cooling system.

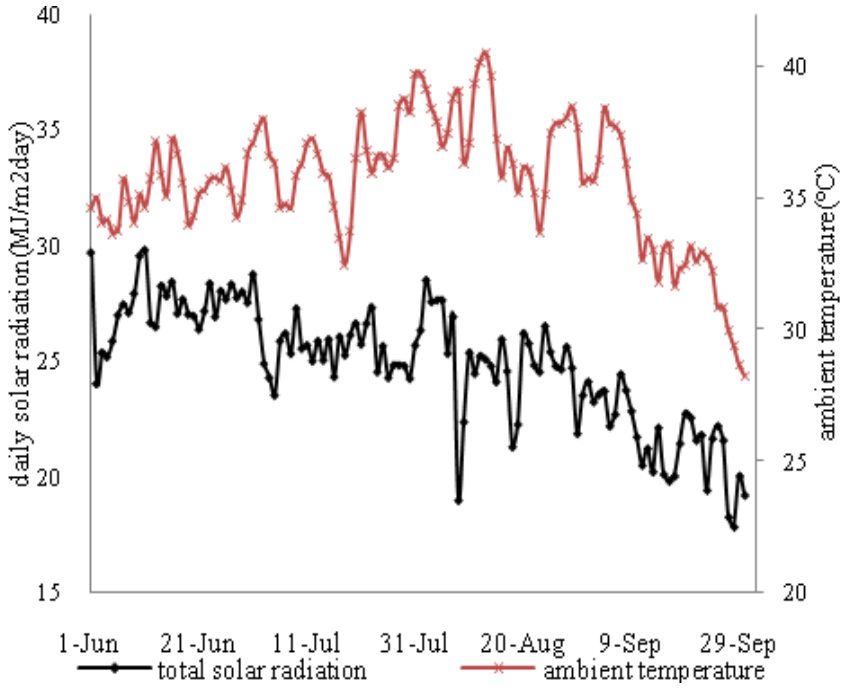

Fig.2. Daily solar radiation and ambient temperature data[14].

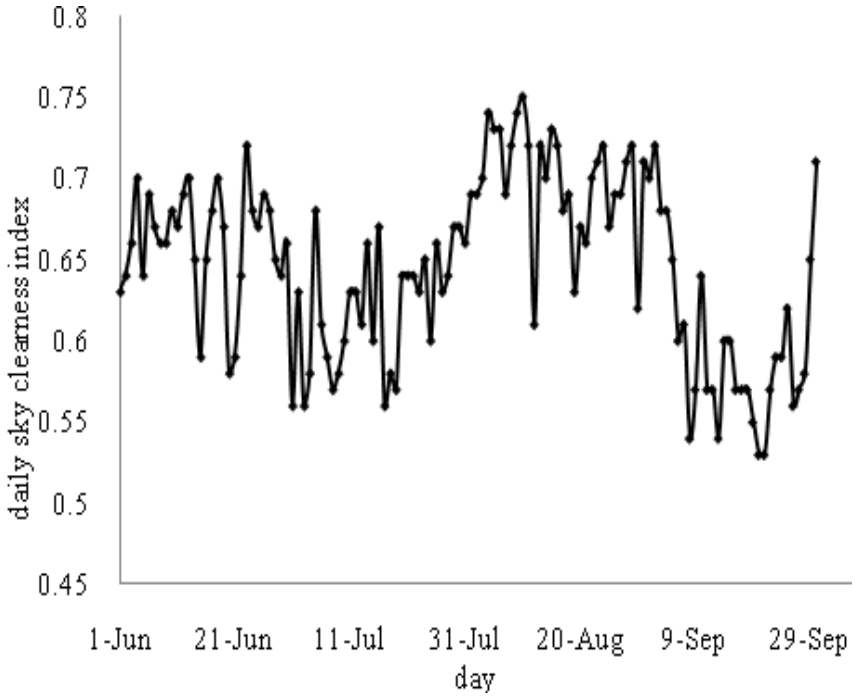

Fig.3. Daily sky clearness index[14].

Daily radiation, ambient temperature and daily sky clearness index for the period of June 1st to September 31st for Ahwaz according to the data provided by IRMO [14] are given in Fig.2 and 3. Collector tilt angle, orientation, collector area and storage tank volume all have importance in system performance.

As a starting point, collector area can be calculated by using the following Eq.(15):

$$A_{sc} = \frac{Q_h}{\eta_c G_{\perp}} \quad (33)$$

For $G_{\perp}$=0.4 kW/m^2 (average radiation for Ahwaz) and η_c=50%, collector area is found to be 55m^2. Since Ahwaz has latitude of 31.31° and the solar system is planned to be used only during summer months, according to [16] the tilt angle of solar collectors are taken as 45° due south. The storage tank volume is sized as a function of collector area using Eq.(34):

$$V = \upsilon A_{sc} \quad (34)$$

where υ is taken to be 50L/m^2 as a starting point according to [13]. Thus V is 2750L for 55m^2 of solar collector. Also the auxiliary heater efficiency is taken as 80%.

Since the adsorption chiller modeled in this study was not. Accessible for writers, the results could not be compared to experimental data for the discussed environmental condition. In order to calculate the optimum values of collector area and tank volume, the LCC of the system is considered as objective function. The optimization was carried out for collector area and tank volume using a MATLAB computer program developed for this purpose. The optimization was carried out using Sequential quadratic programming (SQP) which allows one to calculate the optimal value for constrained problems. LCC is considered as the objective function and is subjected to minimization.

5. Results and Discussion

5.1. Chiller Transient Response

Figure 4 shows the temperature profiles of the hot, cooling and chilled water. After about 700s, the hot water outlet temperature approaches to the inlet temperature, thus the heat consumed by the desorber after this point, will be quite small. But the difference between outlet and inlet temperature for the cooling water is still 2.4°C after 600s of cooling. This difference reaches 0.7°C after cooling the adsorber for 900s which shows that adsorber is sufficiently cooled down and the adsorption ability remains strong until the end of adsorption phase. Therefore the cycle time is taken as 1800s. It is worthy of note that the difference between outlet and inlet temperature of hot water after heating the desorber for 900s is 0.5°C. It is also observed that the outlet temperature of chilled water reaches its minimum after each bed is heated/cooled for 80s. At this point the cooling power is at its maximum and the outlet temperature of chilled water is 11.35°C. The switching time is taken as 30s which is a typical value for adsorption chillers [7,9,10].

Figure 5 shows the temperature profiles of the adsorption beds, condenser, and evaporator.

Figure 6 depicts the cyclic-steady-state dühring diagram simulated by using the mathematical model presented herein. In this figure, the various modes of a complete cycle are designated by numbers: pre-heating mode (1-2), desorption mode (2-3), pre-cooling mode (3-4) and adsorption mode (4-1).

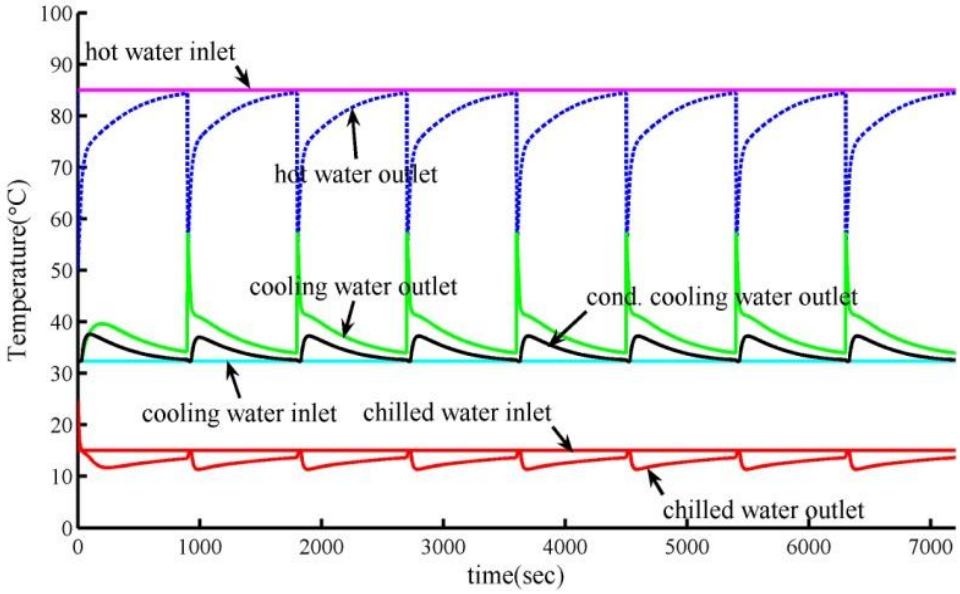

Fig.4. Temperature profiles of hot, cooling and chilled water.

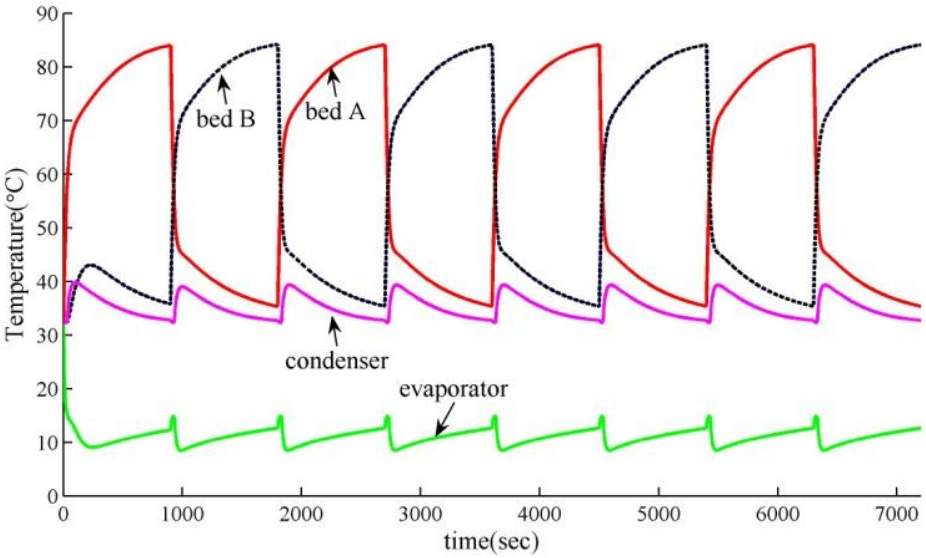

Fig.5. Temperature profiles for adsorption beds, condenser and evaporator.

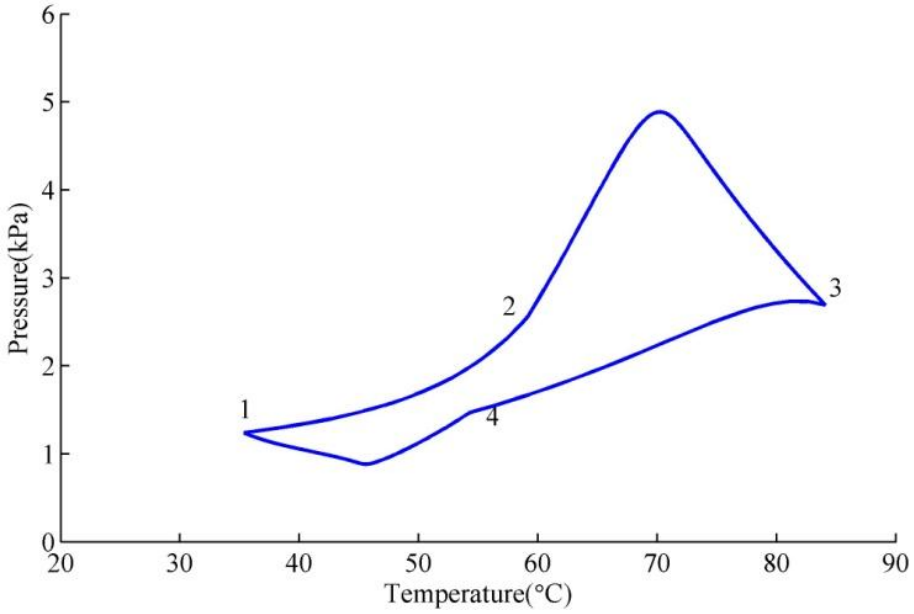

Fig.6. Dühring diagram of the modeled silicagel-water two bed adsorption chiller.

5.2. Solar Hot Water Loop Simulation

The solar energy fluctuation during each day will result in the variation of the storage tank temperature and the heat supplied by the auxiliary heater.

As an example, results for August 10th are shown in Fig.7 and 8. Figure 7 depicts the temperatures of storage tank outlet water, collector outlet water and return water from the desorber. As can be seen from this figure, the temperature of collector outlet water reaches its maximum (92.3°C) around noon. Since the temperature of return water from the desorber follows the profile in Fig.4 it affects the temperature profiles of storage tank outlet water and collector outlet water. This also affects the amount of heat provided by the auxiliary heater which is depicted in Fig.8. From 10:20 am to 14:5 pm the heat provided by the auxiliary heater equals zero, which means during this time solar radiation is the only source of energy in the cooling system.

Useful energy gain of the collector and the energy delivered to the fluid stream by the auxiliary heater are integrated daily and daily average solar fractions and daily auxiliary energy during summer months are illustrated in Fig.9 and 10.

5.3. Effect of Hot Water Temperature

As it is shown in Fig.11, the refrigeration capacity of adsorption chiller increases with increasing the hot water temperature. As for COP, with hot water temperature variation from 65 to 85 °C, COP increases but with further increasing the hot water temperature, COP drops, Because a higher hot water temperature causes a higher heating power as well as a higher refrigerating capacity. For temperatures below 85°C, the increase in heating power is more than the increase in refrigeration capacity thus the optimal hot water temperature is about 85°C for the COP. For temperatures higher than 85°C the increase in heating power is more than the increase in refrigeration capacity, therefore COP decreases.

Increasing hot water temperature results in higher heating power therefore auxiliary heater is required to provide more heat to the adsorption chiller which leads to reduced solar fraction. Figure 12 Shows effect of the hot water temperature on yearly solar fraction and yearly auxiliary heat.

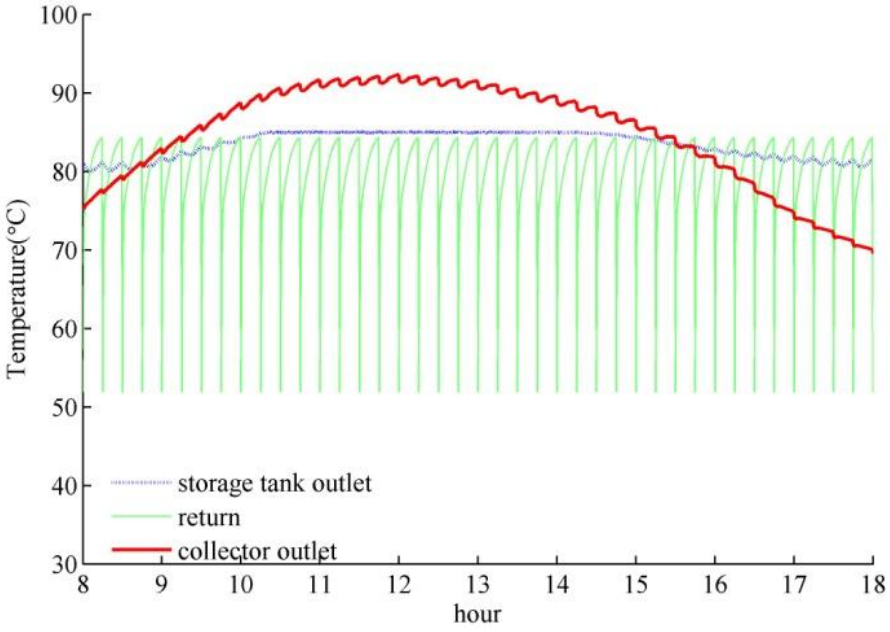

Fig.7. Temperature profiles of collector outlet, tank outlet and return water for August 10th.

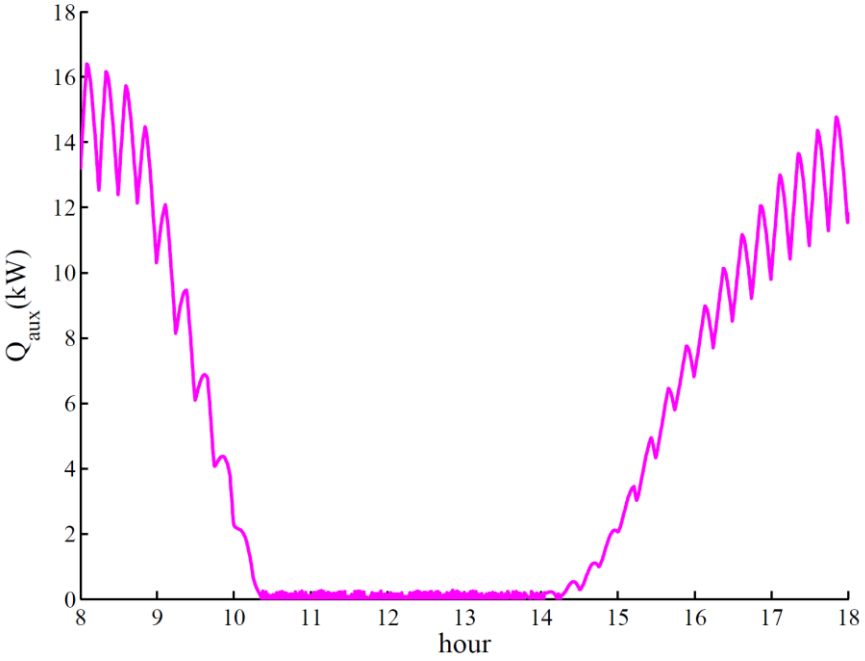

Fig.8. Variations of heat provided by auxiliary heater for August 10th.

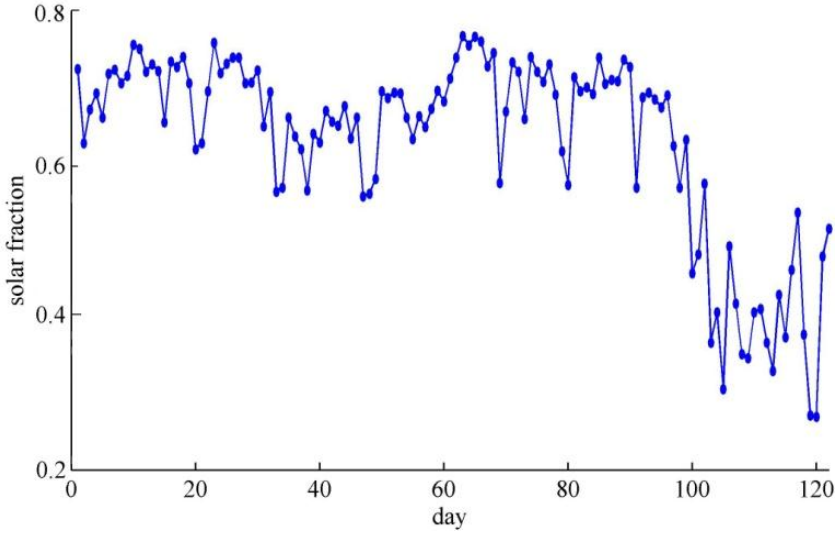

Fig.9. Daily solar fractions (Ac=55m^2, V=2.75m^3).

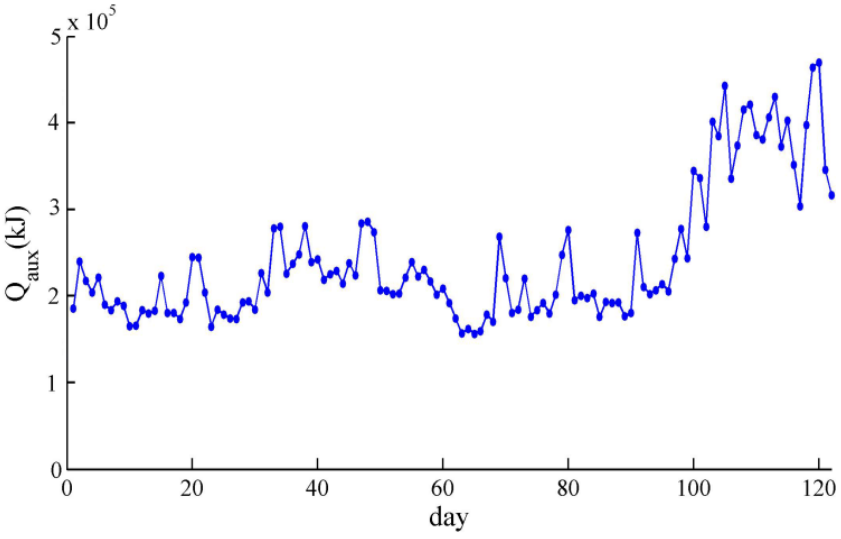

Fig.10. Daily auxiliary heat (Ac=55m^2 and V=2.75m^3)

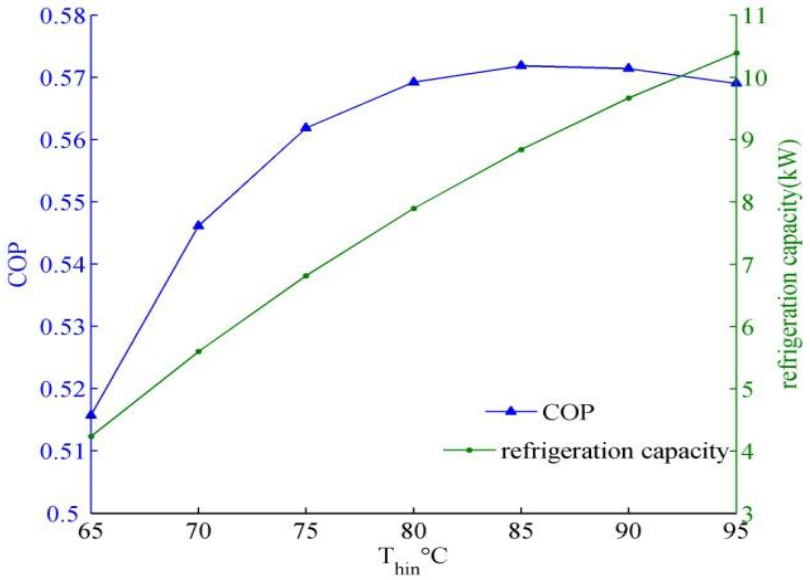

Fig.11. Effect of the hot water temperature on the refrigeration power and COP (cycle time=1800s).

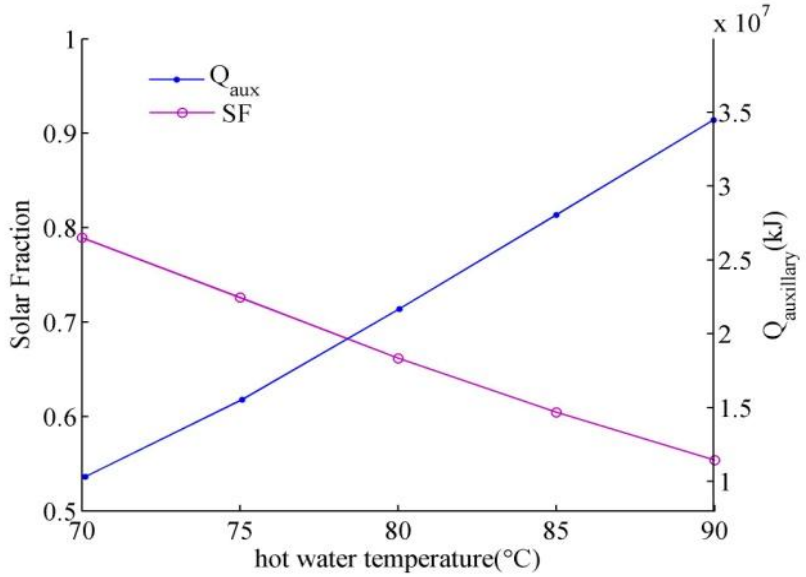

Fig.12. Effect of hot water temperature on yearly SF and Q_{aux} (cycle time=1800s**).**

5.4. Effect of Cycle Time

The refrigeration capacity, COP, yearly solar fraction and auxiliary energy variations with the cycle time are shown in Fig.13 and 14. The COP increases uniformly with extension of the cycle time under a driving heat source of 85°C. This is because a longer cycle time causes much lower consumption of driving heat as well as lower refrigeration capacity, but the decrease in refrigeration capacity is less than that of heating power.

Heating power in each cycle increases with longer cycle times. On the other hand the total number of cycles declines with extending the cycle time. Overall, extending the cycle time results in higher yearly auxiliary heat demand and accordingly lower yearly solar fraction.

5.5. Effect of Switching time

Figures 15 and 16 show how COP, refrigeration capacity, solar fraction and auxiliary heat are affected by the switching time. As can be seen from Fig.15 COP varies slightly with switching time, and reaches a peak value at 40 s. As for refrigeration capacity, the optimal value will be at 30s.

Figure 16 depicts the effect of switching time on solar fraction and yearly auxiliary heat. Heating power increases with extending the switching time therefore the yearly solar fraction increases and yearly heat demand decreases.

5.6. Effect of Collector Area and Storage Tank Volume

The effect of the collector area on the solar fraction is given in Fig.17. As expected, as collector area increases, solar fraction increases and auxiliary heat decreases.

Hot water storage tank volume is also important on the system performance. Storage tank should not be too big since the thermal inertia of the system increases as the storage tank volume increases. On the other hand tank volume should not be too small,

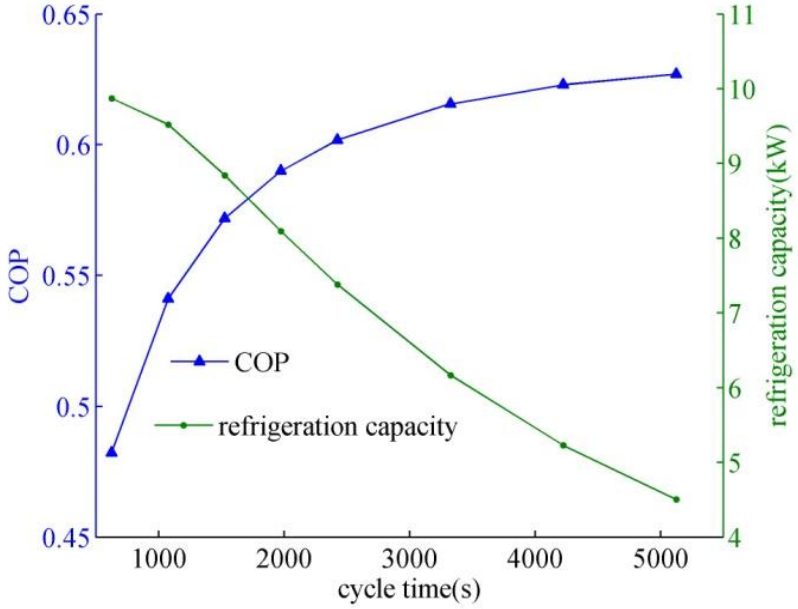

Fig.13. Effect of cycle time on COP and refrigeration capacity (T_{hin}=85C).

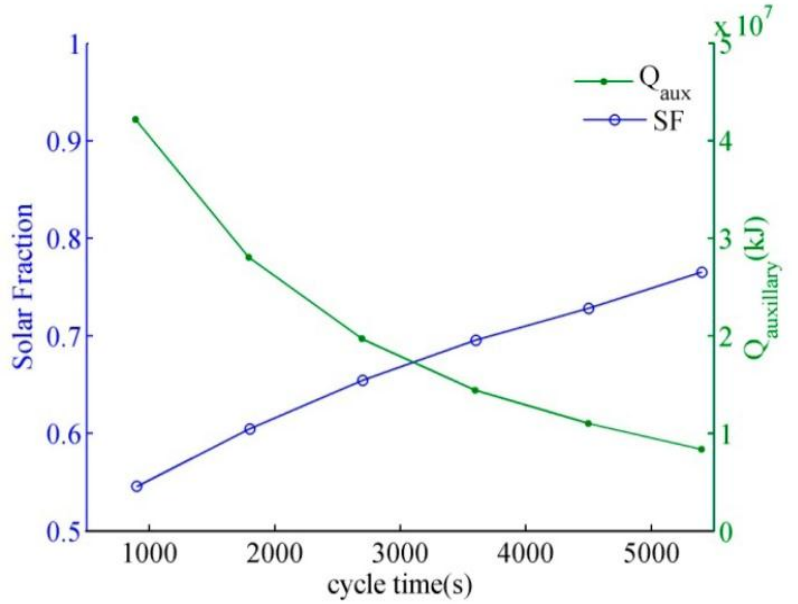

Fig.14. Effect of cycle time on yearly SF and Q_{aux} (T_{hin}=85C).

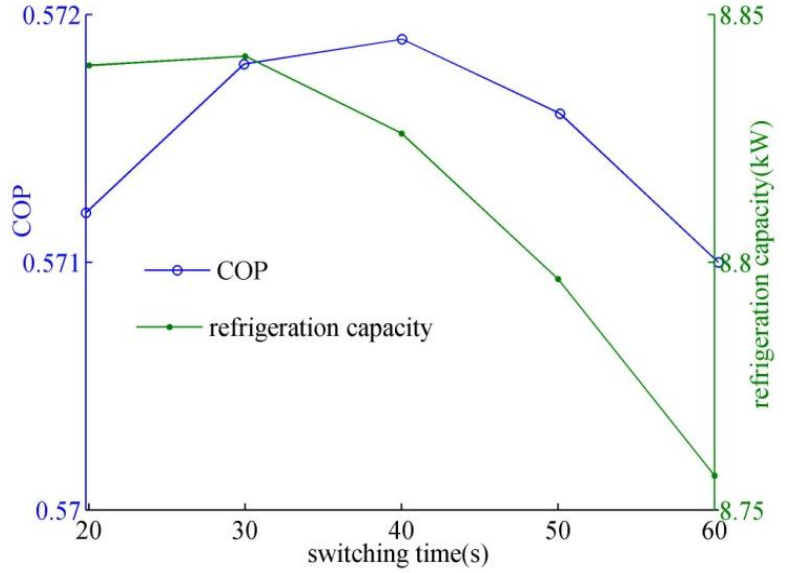

Fig.15. Effect of switching time on COP and refrigeration capacity (cycle time=1800s).

because tank should store enough energy for the times when there is not enough solar radiation for operating the thermal chiller. Figure 18 shows the influence of the storage tank volume on yearly solar fraction and the yearly auxiliary energy demand. As the storage tank volume increases, solar fraction increases and auxiliary heat decreases. As seen from this figure the effect of tank volume on the system performance is much less intense than the effects of hot water temperature, cycle time and collector area.

5.7. Optimization

The initial values for collector area and storage tank volume are taken equal to 55m^2 and 2.75m^3.
As mentioned before, the selection of the tank volume should consider two opposite phenomena: on one hand, an increase of the storage tank volume would determine higher losses, higher capital costs and also a longer response time of the system; on the other hand, larger tank would also allow one to store a greater amount of the energy produced by the solar collector, and consequently to reduce the use of auxiliary energy.

This trade-off results in an optimal value. Also the optimum solar collector area could be considered as the optimal compromise between lower operating costs and higher capital costs due to the increase of the solar collector total surface. The optimum values calculated using the SQP method for collector area and tank volume are:

$$A_c = 38\ m^2, v = 27.5\frac{L}{m^2} \rightarrow V = 1.045 m^3$$

For the optimum design, the solar fraction, auxiliary heat and LCC are 0.49, 35517 MJ and 15705.8$ respectively. Table 2 shows a comparison between the base case and the optimum case.

It is observed that reducing the collector area to 38 m^2 and tank volume to 1.045m^2 leads to a decrease of nearly 11% in life cycle costs of the solar adsorption cooling system.

Table 2. results for optimum and base case

parameter	Optimum case	Base case
A_c(m^2)	38	55
V(m^3)	1.045	2.75
SF	0.49	0.59
Q_{aux}(MJ)	35517	28044
Yearly fuel cost($)	620.49	489.9455
Total fuel cost($)	9944.5	7852.3
Investment cost($)	5761.3	9716.2
LCC($)	15706	17569

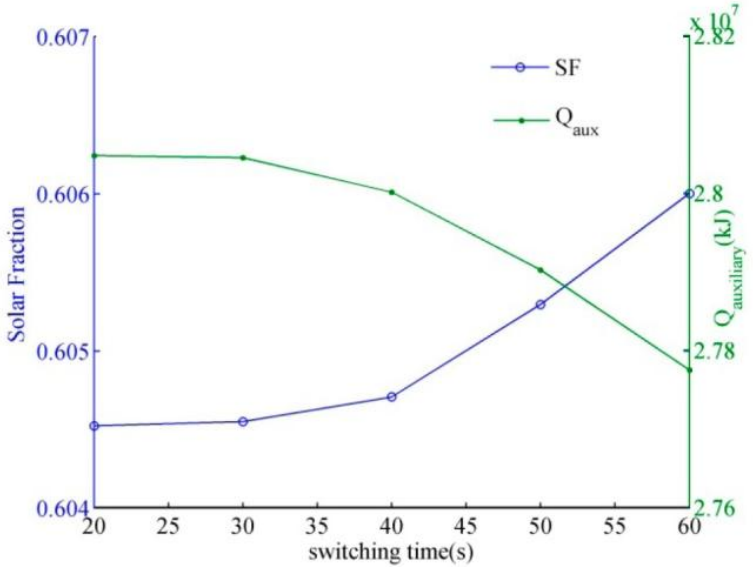

Fig.16. Effect of switching time on yearly SF and Q_{aux} (T_{hin}=85C, cycle time=1800).

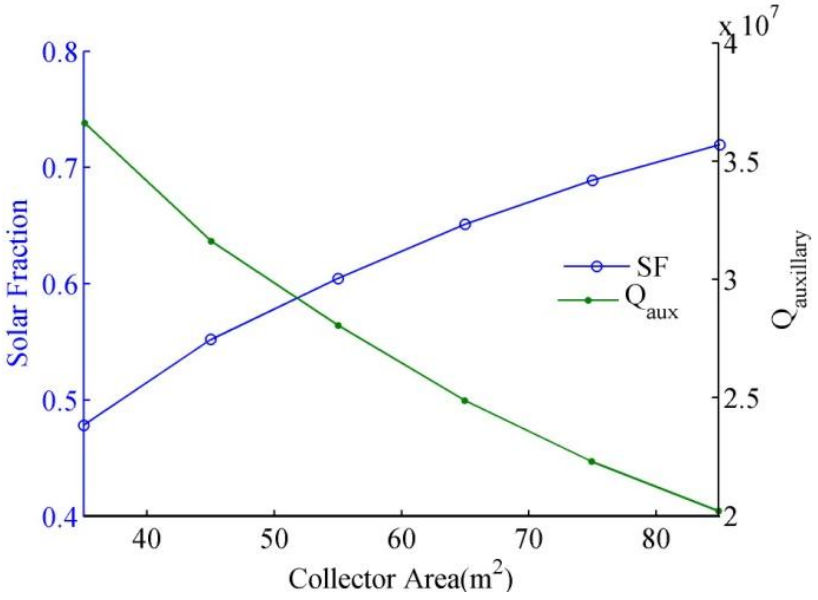

Fig.17. Effect of collector area on yearly SF and Q_{aux}(T_{hin}=85C,cycle time=1800).

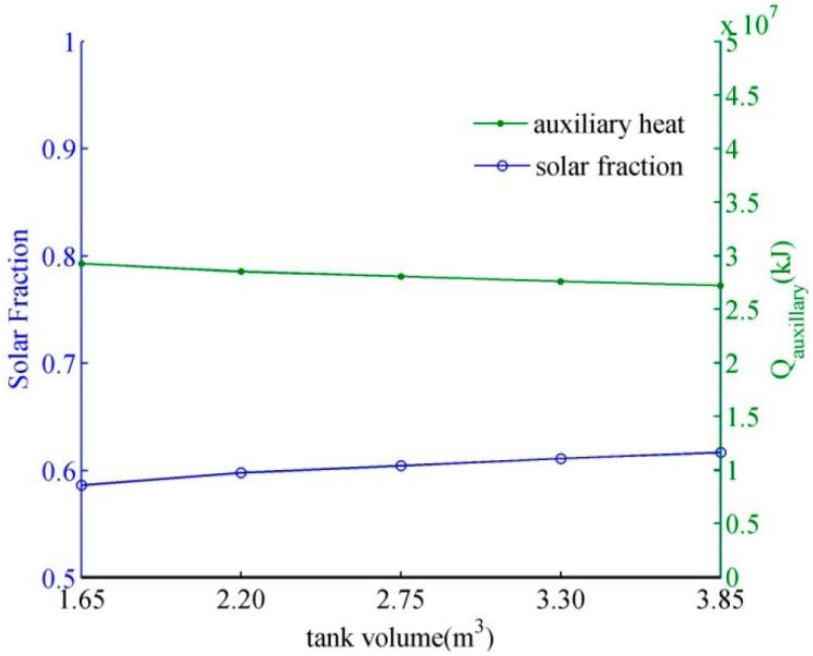

Fig.18. Effect of tank volume on yearly SF and Q_{aux} (T_{hin}=85C, cycle time=1800).

6. Conclusion

In this paper, a complete dynamic model of a solar adsorption cooling system was presented. COP and refrigeration power of the modeled chiller was calculated to be 0.575 and 8.84kW respectively. As a starting point, total collector area used in the solar system was 55m^2 and volume of the storage tank 2750L. Yearly calculated solar fraction and auxiliary heat of this system was 0.62 and 29427MJ respectively. According to the results, the highest and lowest daily solar fractions for the base case occur on August 2nd and September 28th respectively.

Studying the effect of hot water temperature on COP and refrigeration values showed that increasing hot water temperature up to 85°C increased COP but further increasing caused COP to decrease.

For temperatures below 85°C, the increase in heating power is more than the increase in refrigeration but for temperatures higher than 85°C the increase in heating power is more than the increase in refrigeration capacity, therefore COP decreases. It was also observed that refrigeration capacity increased with hot water temperature but decreased significantly with increasing cycle time. Increasing cycle time also improved the COP of the cycle. Furthermore it was demonstrated that the COP and refrigeration capacity vary slightly with switching time. The influence of the mentioned parameters on SF and auxiliary heat was also studied. According to the results, SF decreased with increasing hot water temperature but increased with extending the cycle time and switching time. Auxiliary heat increased with increasing hot water temperature and decreased with increasing the cycle

time as well as switching time due to higher heating power demand. Also studied was the influence of collector area and storage tank volume on SF and auxiliary heat. Results showed that in comparison with tank volume, collector area has much stronger impact on solar fraction and auxiliary heat.

In order to find the optimum values of collector area and storage tank volume, an economic analysis was performed and life cycle costs of the system were calculated for different collector areas and tank volumes. Using SQP method, the optimum configuration was found to be 38m^2 of collector area and 1.045m^3 of tank volume.

Nomenclature

A	Heat transfer area, m^2
c_p	Specific heat, kJ/kgK
COP	Coefficient of Performance
D_{s0}	Surface diffusion, m^2/s
E_a	Activation energy, J/kg
F_R	Collector heat transfer coefficient
H	daily radiation, W/m^2
I	Hourly radiation , W/m^2
L	latent heat of vaporization, kJ/kg
M,m	Mass, kg
$\dot{m}$	Mass flow rate, kg/s
P	Pressure, kpa
R_p	Adsorbent particles radius, m
R	Gas constant, J/kgK
SCP	Specific cooling power
ss	sunset
sr	sunrise
T	Temperature, K
T_0	Ambient temperature, K
t	Time, s
U	Overall heat transfer coefficient, kW/Km^2
x	instantaneous Uptake, kg/kg
x^*	Equilibrium uptake, kg/kg
α	absorptivity
δ	Declination, rad
η	efficiency
θ	Angle of incidence, rad
θ_z	Azimuth angle, rad
λ	Latitude, rad
τ	transmittance
ω	Hour angle, rad
ρ_s	Environmental reflectance

subscripts

a	adsorbent
ad	adsorber
ads	adsorption
Al	aluminum
b	beam
c	condenser
ccw	Condenser Cooling water
chw	Chilled water
cu	cupper
cw	Cooling water
d	diffuse
des	Desorption
e	Evaporator
g	gas
hw	Hot water
in	inlet
lr	return
out	outlet
sc	Solar collector
w	water
wv	Water vapor

References

[1] Wang, R.Z. and Oliveira, R. G. Adsorption refrigeration—An efficient way to make good use of waste heat and solar energy. Progress in Energy and Combustion Science. 2006, Vol. 32, pp. 424–458.

[2] Chemviron, Bruxelles. and Critoph, R.E. An ammonia carbon solar refrigerator for vaccine cooling. Renewable Energy. 1994, Vol. 5, pp. 502–508.

[3] Zeolite based solar refrigerator. Phillip, SK., et al. Gujarat,India : Research Report Sardar Patel Renewable Energy Research Institute., 1993.

[4] Anyanwu, E.E. and Ezekwe, C.I. Design construction and test run of a solid adsorption solar refrigerator using activated carbon/methanol, as adsorbent/adsorbate pair. . Energy Conversion and Management. 2003, Vol. 44, pp. 2879–2892.

[5] Hildbrand, C., et al. A new solar powered adsorption refrigerator with high performance. Solar Energy. 2004, Vol. 77, 3, pp. 311–318.

[6] Wang, D.C., et al. Study of a novel silica gel–water adsorption chiller. Part I. Design and performance prediction. International Journal of Refrigeration. 2005, Vol. 28, pp. 1073–1083.

[7] Chuaa, H.T., et al. Modeling the performance of two-bed, sillica gel-water adsorption chillers. International Journal of Refrigeration. 1999, 22, pp. 194–204.

[8] Wang, Xiaolin and Chua, H.T. Two bed silica gelewater adsorption chillers: An effectual lumped parameter model. International Journal of Refrigeration. 2007, Vol. 30, pp. 1417-1426.

[9] Saha, B. B., et al. 'Study on an activated carbon fiber ethanol adsorption chiller: Part I- system description and modelling. International Journal of Refrigeration. 2007, Vol. 30, pp. 86 – 95.

[10] Boelman, E.C., Saha, B.B. and Kashiwagi, T. Computer simulation of a silica gel–water adsorption refrigeration cycle—the influence of operating conditions of cooling output and COP. ASHARE Transactions. 1995, pp. 348–355.

[11] Chihara K, Suzuki M. Air drying by pressure swing adsorption. Journal Of Chemical Engineering Of Japan. 1983, Vol. 16, 4, pp. 293–299.

[12] Duffie, J. A. and Beckman, W. A. Solar Engineering of Thermal Process. Wisconsin: John Wiley& Sons Inc., 1991.

[13] Calise, F., d'Accadia, M., Dentice and Vanoli, L. Thermoeconomic optimization of Solar Heating and Cooling systems. Energy Conversion and Management. 2011, Vol. 52, pp. 1562–1573.

[14] IRMO. Iran Metrological Organization. [Online] http://www.irimo.ir.

[15] Henning, H.M. Solar assisted air-conditioning in buildings, A handbook for planners. 2nd edition. Wien: Springer-Verlag, 2007.

[16] Gunerhan, H. and Hepbaslı, A. Determination of the optimum tilt angle of solar collectors for building applications. Building and Environment. 2007, 42, pp. 779 –783.